Analysis of Arbitrarily Shaped Dielectric Lens Antenna by Ray Tracing Method

Mitsuo TAGUCHI*, Kosuke UCHIUMI**, Hideaki SHIMODA*** and Kazumasa TANAKA

Dept. of Electrical & Electronic Eng., Nagasaki University
** Graduate School of Science and Technology, Nagasaki University
1-14 Bunkyo-machi, Nagasaki-shi, 852-8521, Japan
*** Technical Center, TDK Co.
2-15-7, Higashi-Ohwada, Ichikawa-shi, Chiba, 272-0026 Japan
E-mail: mtaguchi@net.nagasaki-u.ac.jp

Introduction

The authors have reported the three dimensional ray tracing method for the analysis of dielectric lens antenna with arbitrarily shaped inner and outer surface [1], [2]. In these papers, however, the multiple reflections are not considered. In this paper, the ray tracing method is applied to the dielectric lens antenna. The primary radiator of this lens antenna is the H-sectral horn fed by the rectangular waveguide [3]. The multiple reflection of ray is considered.

Formulation

Figure 1 shows the dielectric lens antenna and the coordinate system for the ray tracing method [1], [2]. $\boldsymbol{i}_x$, $\boldsymbol{i}_y$ and $\boldsymbol{i}_z$ are the unit vectors of the Cartesian coordinate system. Let the source point on the primary radiator be $P_0(x_0, y_0, z_0)$. The equivalent electric and magnetic currents $J_y(x_0, y_0)\boldsymbol{i}_y$ and $M_x(x_0, y_0)\boldsymbol{i}_x$ are assumed on the source point P_0. The inner surface of lens is S_1, the outer surface of lens is S_2 and the reference plane of lens antenna is S_3. The points of the ray on S_1, S_2 and S_3 are defined as $P_1(x_1, y_1, z_1)$, $P_2(x_2, y_2, z_2)$ and $P_3(x_3, y_3, z_3)$, respectively. $R_\nu = \overline{P_{\nu-1}P_\nu}$ is the distance between two points $P_{\nu-1}$ and P_ν (ν=1,2,3), and $\mathbf{i}_\nu$ is the unit vector from $P_{\nu-1}$ to P_ν.

Snell's law is expressed as follows:

$$k_1 \sin\theta_1 = k_2 \sin\theta_2. \tag{1}$$

Where k_1 and k_2 are the propagation constants within the outside and inside region of lens, and θ_1 and θ_2 are the incident and the refractive angles, respectively. Applying Eq. (1) to the ray tracing method, we obtain

$$\mathbf{i}_{\nu+1} = \frac{1}{n'}\mathbf{i}_\nu + \mathbf{n}_\nu \left[\sqrt{1 - \frac{1}{(n')^2}\left\{1 - (\mathbf{i}_\nu \cdot \mathbf{n}_\nu)^2\right\}} - \frac{1}{n'}\mathbf{i}_\nu \cdot \mathbf{n}_\nu \right]. \tag{2}$$

Where n is the refractive index of lens.

$$n = \frac{k_2}{k_1} = \sqrt{\frac{\mu_2}{\mu_1}} \sqrt{\frac{\varepsilon_2 - j(\sigma_2/\omega)}{\varepsilon_1 - j(\sigma_1/\omega)}}, \quad n' = \begin{cases} n & (\nu = 1) \\ \dfrac{1}{n} & (\nu = 2) \end{cases} \tag{3}$$

Applying Eq. (2) to the ray tracing method, the points P_1, P_2 and P_3 on S_1, S_2 and S_3 can be obtained straightforwardly.

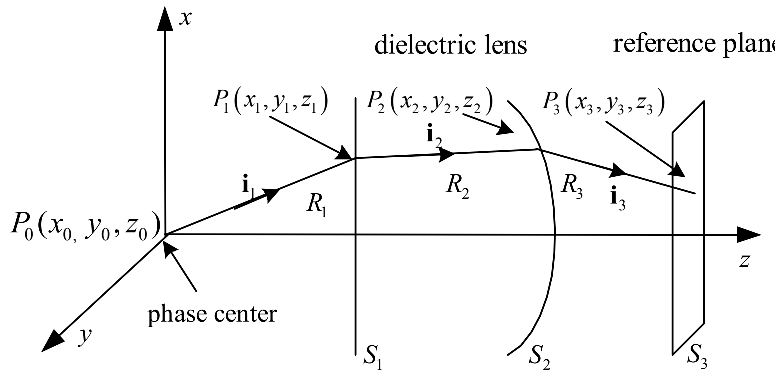

Figure 1. Coordinate system for ray tracing method

Fresnel's transmission coefficients of parallel and perpendicular polarization are given by the following expressions.

(a) Parallel polarization

$$T_{TM} = \frac{2\mu_2 n \cos\theta_1}{\mu_1 n^2 \cos\theta_1 + \mu_2 \sqrt{n^2 - \sin^2\theta_1}} \tag{5}$$

(b) Perpendicular polarization

$$T_{TE} = \frac{2\mu_2 \cos\theta_1}{\mu_2 \cos\theta_1 + \mu_1 \sqrt{n^2 - \sin^2\theta_1}} \tag{6}$$

By using Eqs. (1), (3) - (5), the incident electric field at P_1 is expressed as follows.

$$\boldsymbol{E}_{P_1}^{in} = \left(E_{P_1}^{x} \boldsymbol{i}_x + E_{P_1}^{y} \boldsymbol{i}_y + E_{P_1}^{z} \boldsymbol{i}_z \right) \psi \tag{7}$$

$$E_{P_1}^{x}(x_1, y_1) = \frac{k_1^2}{4\pi R_1^2}(x_1 - x_0)(y_1 - y_0) J_y(x_0, y_0) \tag{8}$$

$$E_{P_1}^{y}(x_1, y_1) = \frac{1}{4\pi}\left[\left\{ \frac{k_1^2}{R_1^2}(y_1 - y_0)^2 - j\omega\mu_0 \right\} J_y(x_0, y_0) + \frac{jk_1}{R_1}(z_1 - z_0) M_x(x_0, y_0) \right] \tag{9}$$

$$E_{P_1}^{z}(x_1, y_1) = \frac{1}{4\pi}\left\{ \frac{k_1^2}{R_1^2}(y_1 - y_0)(z_1 - z_0) J_y(x_0, y_0) - \frac{jk_1}{R_1}(y_1 - y_0) M_x(x_0, y_0) \right\} \tag{10}$$

$$\psi = \frac{\exp(-jkR_1)}{R_1} \tag{11}$$

The electric field on the reference plane S_3 is obtained as,

$$\boldsymbol{E}_{P_3} = \left(E_{P_3}^{x} \boldsymbol{i}_x + E_{P_3}^{y} \boldsymbol{i}_y + E_{P_3}^{z} \boldsymbol{i}_z \right) \psi \tag{12}$$

$$\begin{aligned} E_{P_3}^{i}(x_3, y_3) &= \left\{ K_x^i E_{P_1}^{x}(x_1, y_1) + K_y^i E_{P_1}^{y}(x_1, y_1) + K_z^i E_{P_1}^{z}(x_1, y_1) \right\} \\ &\times \frac{\exp\{-j(k_1 R_1 + k_2 R_2 + k_1 R_3)\}}{R_1 R_2 R_3}, \qquad i = x, y, \text{or } z \end{aligned} \tag{13}$$

$$R_1 = \overline{P'P_1}, \quad R_2 = \overline{P_1 P_2}, \quad R_3 = \overline{P_2 P_3}$$

K_x^i, K_y^i, K_z^i denote the variables defined by the normal vectors and the transmission coefficients at the points P_1 and P_2. The transmission coefficient at each point depends on the mode of incident ray. In the calculation of the electric field, the multiple reflections are also considered.

The radiation field is calculated by the surface integral on the reference plane S_3. Replacing the coordinate origin to the point of intersection of S_3 and the z-axis, the electric field is expressed by

$$\begin{aligned} \boldsymbol{E}(r,\theta,\phi) &= \frac{1}{4\pi}\int_{S_3}\left\{-j\omega\mu\psi(\boldsymbol{n}'\times\boldsymbol{H})+(\boldsymbol{n}'\times\boldsymbol{E})\times\nabla'\psi+(\boldsymbol{n}'\cdot\boldsymbol{E})\nabla'\psi\right\}dS' \\ &= \frac{\exp(-jkr)}{r}\boldsymbol{D}(\theta,\phi) \end{aligned} \tag{14}$$

$$\begin{aligned} \boldsymbol{D}(\theta,\phi) = \frac{jk_1}{4\pi}\int_{S_3}\Big[&\left\{E_{P_3}^{x}(x_3,y_3)\cos\phi+E_{P_3}^{y}(x_3,y_3)\sin\phi\right\}\boldsymbol{i}_\theta-\left\{E_{P_3}^{x}(x_3,y_3)\cos\theta\sin\phi\right. \\ &\left.-E_{P_3}^{y}(x_3,y_3)\cos\theta\cos\phi\right\}\boldsymbol{i}_\phi\Big]\exp\left\{jk_1\left(x_3\sin\theta\cos\phi+y_3\sin\theta\sin\phi\right)\right\}dS' \end{aligned} \tag{15}$$

Numerical and experimental results

Figure 2 shows the structure of dielectric lens antenna [3]. The primary radiator is the H-sectral horn fed by the rectangular waveguide. The width of H-sectral horn is $W = 4.5mm$. The dielectric lens of relative permittivity 2.1 is located at the aperture of horn antenna. Figure 3 shows the example of the locus of ray. Figure 4 shows the electric field radiation patterns at frequency 59.6 GHz. The calculated patterns are compared with the measured results [3]. Figure 5 shows the frequency characteristics of electric field radiation patterns.

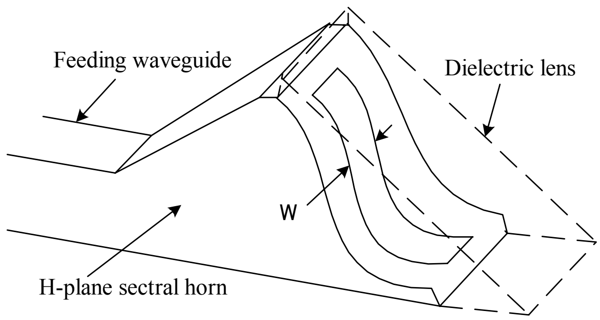

Figure 2. Geometry of dielectric lens antenna

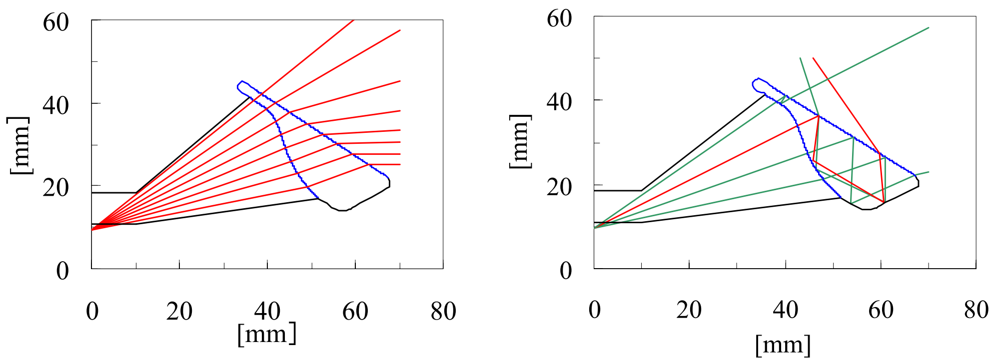

(a) without multiple reflections (b) multiply reflected rays

Figure 3. Locus of ray

Conclusion

The three dimensional ray tracing method for the dielectric lens antenna has been presented. The multiple reflections have be considered in this method. The radiation pattern of the dielectric lens antenna has be calculated by the ray tracing method. This ray tracing method is applicable to the dielectric lens antenna with nonsymmetrical inner and outer surface. Now the radiation patterns of the dielectric lens antenna with the matching layers on the lens surfaces are calculating.

References

[1] M. Taguchi, M. Masuda, H. Shimoda and K. Tanaka, "Analysis of arbitrarily shaped dielectric lens antenna", Proc. of IEEE AP-S Int. Symp., vol.2, pp.769-772, July 2001.

[2] M. Taguchi, M. Igasaki, H. Shimoda, K. Tanaka: Proc. of IEEE AP-S Int. Symp., vol. 3, 109.2, June 2003.

[3] A. Kezuka and Y. Yamada, "Analysis of electrical fields in a lens horn antenna using FDTD method", Technical Report of IEICE, AP2003-254, Jan. 2004.

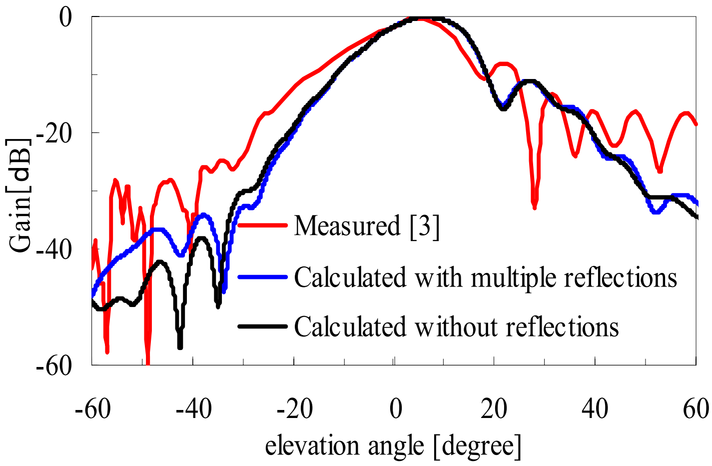

Figure 4. The electric field radiation pattern

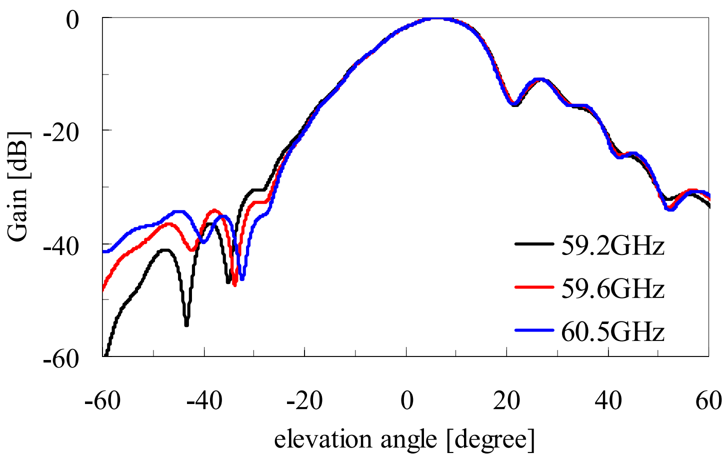

Figure 5. The variation of electric field radiation pattern